metals

MDPI

Article

Research on the Micro-Extrusion Process of Copper T2 with Different Ultrasonic Vibration Modes

Linhong Xu [1], Yulan Lei [1], Haiou Zhang [2], Zhaochen Zhang [1], Yuchu Sheng [1] and Guangchao Han [1,3,4,*]

1 Faculty of Mechanical & Electronic Information, China University of Geosciences, Wuhan 430074, China; xulinhong@cug.edu.cn (L.X.); leiyulanan@163.com (Y.L.); marks_zhang93@163.com (Z.Z.); lll635073228@163.com (Y.S.)
2 School of Mechanical Science & Engineering, Huazhong University of Science and Technology, Wuhan 430074, China; zholab@hust.edu.cn
3 State Key Laboratory of Mechanical System and Vibration, Shanghai Jiao Tong University, Shanghai 200240, China
4 Shanxi Key Laboratory of Non-Traditional Machining, Xi'an Technological University, Xi'an 710032, China
* Correspondence: hgc009@cug.edu.cn; Tel.: +86-189-8612-5967

Received: 8 October 2019; Accepted: 6 November 2019; Published: 10 November 2019

Abstract: As an effective method for the fabrication of miniature metallic parts, the development of micro-forming process (MFP) is still restricted by the existence of size effect. To improve the micro-forming performance of metal material, ultrasonic vibration assisted MFP had been studied extensively for its superiorities in improving materials flow stress and reducing interfacial friction. However, from the literature available, the high frequency vibration was usually found to be superimposed on the forming tool while seldom on the workpiece. Our group developed a special porous sonotrode platform which can realize tool vibration and workpiece ultrasonic vibration independently. In this work, ultrasonic micro-extrusion experiments for copper T2 material under tool vibration and the workpiece vibration condition, respectively, were conducted for comparing the micro-forming characteristic of different vibration modes. The micro-extrusion experiment results of copper T2 show that the lower extrusion flow stress, the higher micro-extrusion formability and surface micro-hardness, and more obvious grain refinement phenomenon can be obtained under the workpiece vibration condition compared with that of tool vibration. These findings may enhance our understanding on different ultrasonic forming mechanisms and energy transmission efficiency under two different vibration modes.

Keywords: copper T2; ultrasonic vibration mode; micro-extrusion; tool vibration; workpiece vibration; energy transmission

1. Introduction

Micro-forming process (MFP) has attracted extensive attention in the manufacturing of micro metallic parts, which has been widely applied in aerospace, micro-electromechanical systems, medical science and other fields [1,2]. However, the development micro-plastic forming technology is still restricted by the existence of size effect which resulting the poor micro-forming performance. In recent years, many researchers have found that the superposition of ultrasonic vibration on MFP was an effective way to change the interfacial friction condition, reduce the forming force and surface roughness during the micro-forming process.

Hu et al. studied the ultrasonic micro compression process of pure aluminum with a dynamic impact effect [3]. Lou et al. investigated ultrasonic micro-extrusion formability of the ZK60 magnesium at room temperature [4]. Yao et al. studied the effects of superimposing high-frequency vibration on the micro upsetting of aluminum [5]. Hung et al. applied ultrasonic vibration to the micro-upsetting of brass alloy [6]. Bai and Yang introduced vibration-assisted micro-forging to improve the surface finishing of metal foils [7]. From the literature available, we found that the ultrasonic vibration in MFP was mostly superposed on the forming tool, which was usually integrated designed with the ultrasonic system. On the other hand, it was shown that the ultrasonic vibration of workpiece could also change the plastic forming properties of material and generate an ultrasonic softening effect on the whole material during the plastic forming process [8]. Yusof Daud et al. studied ultrasonic compression tests of aluminum with workpiece vibration by double slotted block horn and inverted ultrasonic system [9]. Cristina Bunget realized an ultrasonic micro-extrusion process with workpiece vibration by special designed inverted ultrasonic supporting system [10]. Similar special designed inverted ultrasonic supporting systems were also applied in ultrasonic tension [11] and ultrasonic compression [12,13] processes with workpiece vibration. It could be found that the ultrasonic vibration was more difficult to be superimposed on the workpiece vibration comparing with the tool vibration, which was usually applied with special designed ultrasonic system and supporting system. This is mainly because the vibration characteristics of ultrasonic system should be easily affected by the random weight and shape of the workpiece, while the fixed structure of forming tool could be easily applied with ultrasonic resonant vibration.

However, far little attention has been paid on the different ultrasonic forming mechanism between tool vibration and workpiece vibration, which is important to give full play to the advantages of ultrasonic vibration in MFP. In this paper, a self-developed porous block sonotrode system was used to realize ultrasonic resonant vibration with tool or workpiece without any more modification on extrusion equipment. Furthermore, the ultrasonic micro-extrusion process of copper T2 under tool vibration and workpiece vibration were studied respectively to investigate the micro-forming mechanism of different ultrasonic vibration modes. The micro-formability, micro-extrusion stress-strain characteristics, micro-hardness and grain refinement property of material were analyzed to evaluate the different ultrasonic forming performance.

2. Materials and Methods

2.1. Experimental Set-Up

To analyze the ultrasonic micro-forming characteristics of different ultrasonic vibration modes, the ultrasonic vibration of micro-forming tool or workpiece would better be superimposed with the same ultrasonic system. To fit for this special requirement, a self-developed 19.5 kHz ultrasonic vibration system was designed to excite the tool or workpiece respectively [14,15]. The ultrasonic vibration system included a TJS-3000 ultrasonic generator, two YP5020-4D ultrasonic transducers, two step ultrasonic horns (which were all from Hangzhou Successful Ultrasonic Equipment Co. Ltd, Hangzhou, China), and a special self-developed porous sonotrode. The porous sonotrode could transfer the horizontal input vibration of ultrasonic transducers to vertical output vibrations, and the tool or workpiece could make vertical ultrasonic resonant vibration with the porous sonotrode (shown in Figure 1).

Based on the 19.5 kHz ultrasonic vibration system, a 10 kN ultrasonic-assisted plastic forming press machine had also been developed to match the flexible realization of ultrasonic tool vibration or workpiece vibration, as shown in Figure 2 [16]. When the micro-forming tool was fixed on the central of porous sonotrode, the ultrasonic vibration system could be set up on the top board of the machine and the ultrasonic MFP with tool vibration could be realized (shown in Figure 2a). On the other hand, when the workpiece and micro-forming mold were fixed on the central of porous sonotrode, the ultrasonic vibration system could be set up on the lower platen of the machine and the ultrasonic MFP with workpiece vibration could also be realized (shown in Figure 2b).

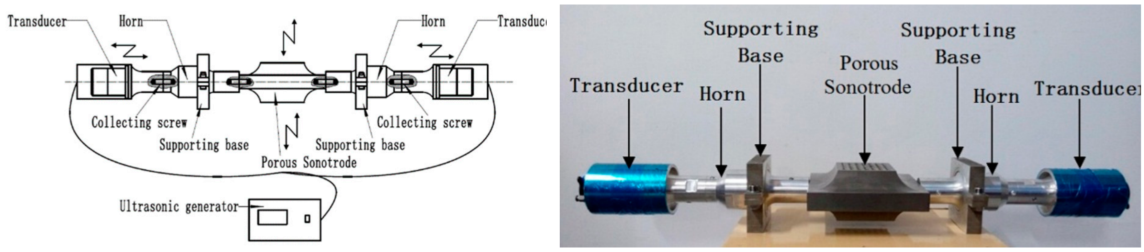

(**a**) (**b**)

Figure 1. Schematic diagram (**a**) and picture (**b**) of ultrasonic system with porous sonotrode [14].

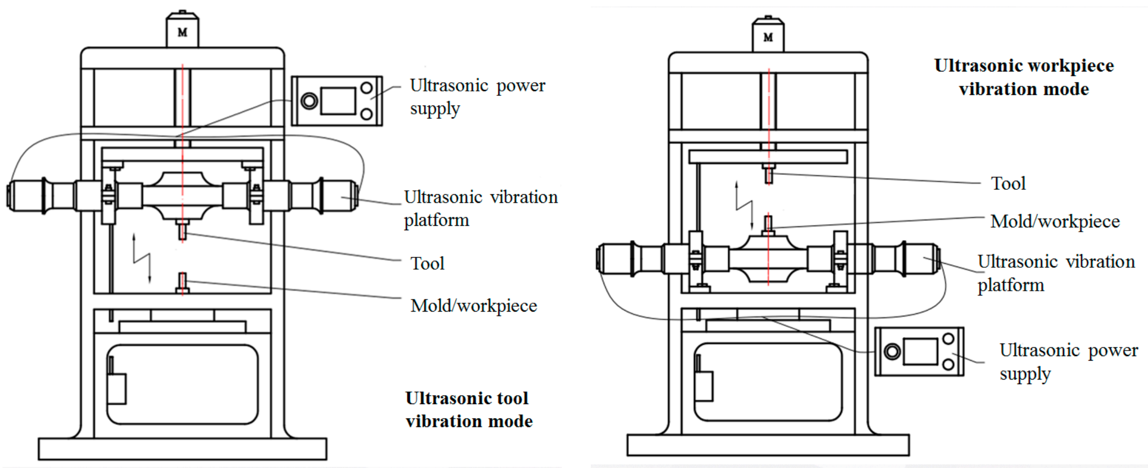

(**a**) tool vibration mode (**b**) workpiece vibration mode

Figure 2. The scheme diagram of ultrasonic plastic forming press machine with different vibration modes.

2.2. Specimens and Mold

T2 copper specimens were used in micro-extrusion experiments. The T2 copper wire with 1.5 mm diameter was firstly prepared by heat treatment processes under different temperatures to obtain different initial grain sizes L (L represents the grain size), such as L = 21, 147 and 230 μm, as shown in Figure 3. Then the copper wire was polished and sectioned into ϕ 1.2 mm × 1.2 mm cylindrical specimens. Furthermore, the split micro-extrusion molds were designed and manufactured with ϕ 0.5 mm V-shaped cone extrusion section to reflect micro-extrusion characteristic of whole extrusion process, as shown in Figure 4a,b. In addition, the simulated ultrasonic vibration modals (mold or tool supported by the ultrasonic vibration system) are shown in Figure 4c,d. It is clear that resonant frequency of the ultrasonic vibration system fluctuated from 19,091 Hz to 19,345 Hz with different loadings of tool and mold, which is within the working range of ultrasonic generation and without any adjustment of ultrasonic system.

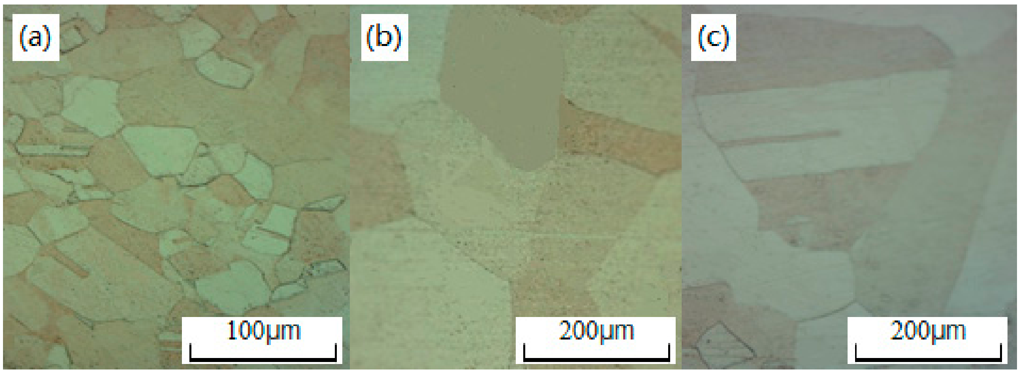

600 °C, 12 h 650 °C, 24 h 800 °C, 24 h

Figure 3. Microscopic microstructure of heat-treated specimen with different grain sizes.

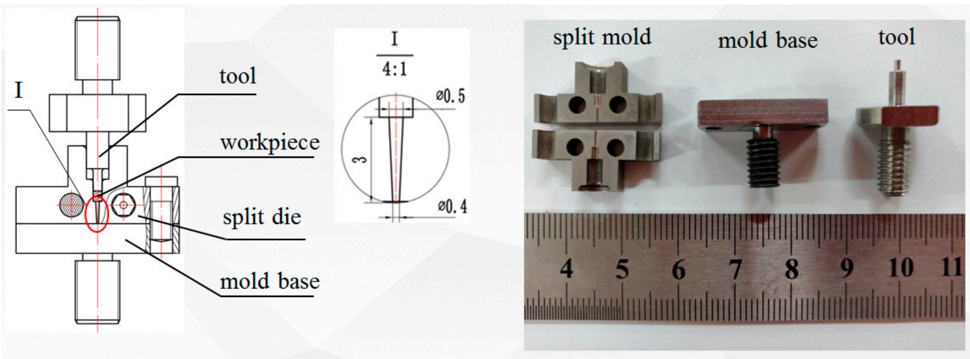

(**a**) scheme diagram of mold (**b**) picture of mold and tool

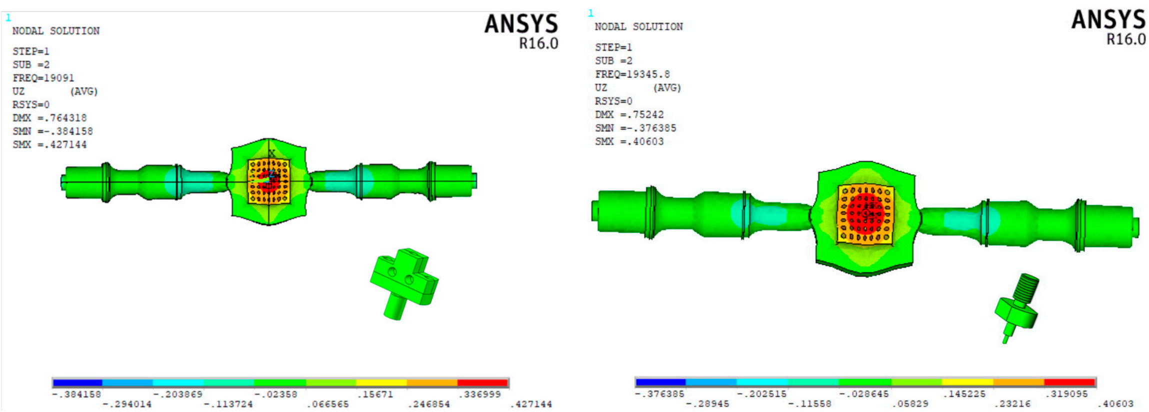

(**c**) simulated workpiece vibration modals (**d**) simulated tool vibration modals

Figure 4. The structure of micro forming molds/tools (**a**,**b**) and the simulated ultrasonic vibration modals(**c**,**d**).

2.3. Experimental Procedure

During the experiments, the vertical ultrasonic resonant vibration of tools or workpieces was realized by screwing the micro-extrusion tool or the mold together with the center of the porous sonotrode respectively. The copper specimen was placed in the mold and pre-compressed between the tool and mold under 200 N to ensure the contact between tool and workpiece and finally reach a stable ultrasonic vibration state before the ultrasonic generator was turned on. Then the micro-extrusion tool continued to press down for another 1 mm distance and complete the ultrasonic micro-extrusion process. The ultrasonic power outputs of ultrasonic generator were set from 0, 35%, 65% to 95%, while the corresponding ultrasonic vibration amplitudes of the forming tool were 0, 3.5 μm, 5.5 μm and 9.2 μm, and the corresponding ultrasonic vibration amplitudes of mold were 0, 2.5 μm, 5.0 μm and 8 μm respectively. Ultrasonic vibration amplitudes of tool and mold were measured by LK-H020 laser measuring instrument of Keyence, Japan. A series of static and ultrasonic micro-extrusion experiments under different ultrasonic vibration modes were performed with a constant extrusion speed of 0.2 mm/min under dry surface condition. The influence of vibration modes, ultrasonic power output and grain size of copper T2 was studied in the micro-extrusion processes. After the experiment, the copper specimens were observed by OLYMPUS-BX61 (OLYMPUS, Beijing, China) electron microscopy and tested by using HV-1000A micro-hardness tester of Laizhou Huayin Test Instrument Co. LTD, Laizhou, China.

3. Results

3.1. Effect of Ultrasonic Power Output and Vibration Modes

The results of true stress and true strain of different ultrasonic power outputs and different vibration modes are shown in Figure 5; Figure 6. Take the specimen with 21 μm grain for example, the true stress of micro-extrusion decreased with the increase of ultrasonic power output on the whole. When the output of ultrasonic power increased to 95%, a maximum reduction of 42.63% and 48.05% was reached, respectively, under tool vibration and workpiece vibration (as shown in Figure 5a,b). Furthermore, the maximum true stress of workpiece vibration was 9.46% lower than that of tool vibration when the ultrasonic power output reached 95% (shown in Figure 6a). Similar trends can be also found in other specimens with grain sizes of 147 μm and 230 μm (as shown in Figures 5c–f and 6b,c)

On the other hand, the results of micro extrusion length under different ultrasonic power outputs and different vibration modes are shown in Figures 7 and 8. It appears that the micro-extrusion lengths increased with the increasing ultrasonic power output (shown in Figure 8a,b), where in ΔH (Increment of extrusion length basing on the static extrusion length, as shown in Figure 7) of 21 μm specimen is 1.74 mm under tool vibration and 2.48 mm under workpiece vibration respectively when the ultrasonic power output is increased to 95% (as shown in Figure 7a,b). It also means that the micro-extrusion length of workpiece vibration is 42.53% longer than that of tool vibration with the 95% ultrasonic power output (shown in Figure 8c). Figures 7c–f and 8d,e also show the similar trends about 147 μm and 230 μm specimen.

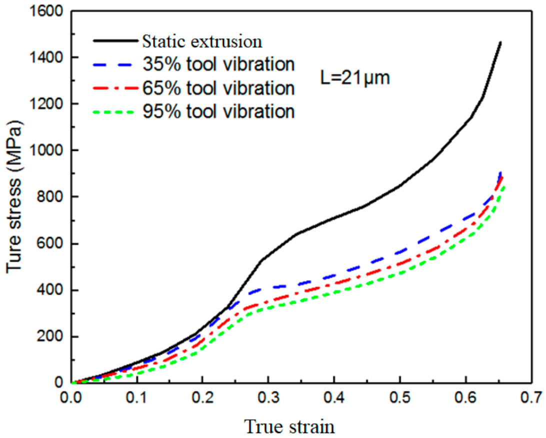

(**a**) Tool vibration mode of 21 μm grain

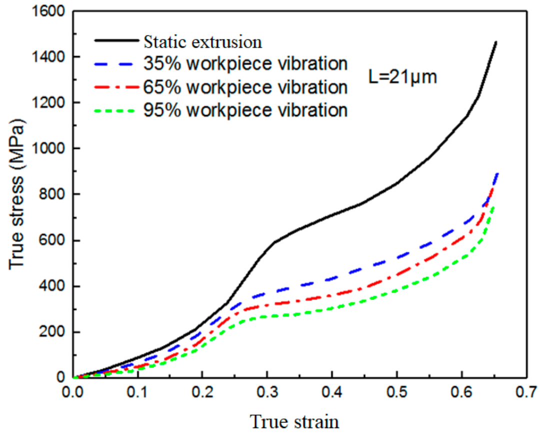

(**b**) Workpiece vibration mode of 21 μm grain

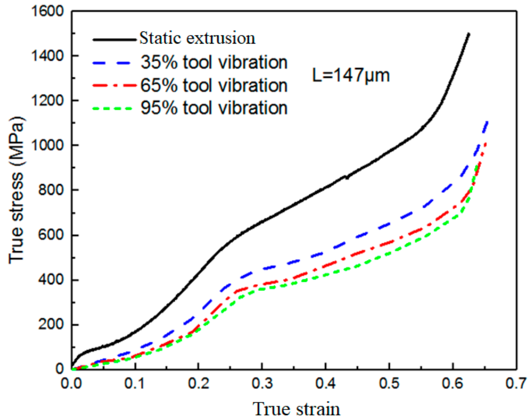

(**c**) Tool vibration mode of 147 μm grain

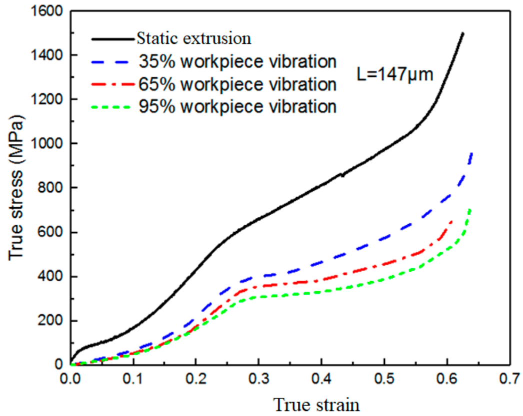

(**d**) Workpiece vibration mode of 147 μm grain

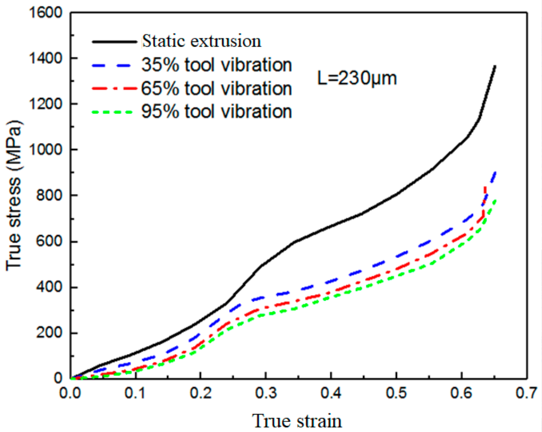

(**e**) Tool vibration mode of 230 μm grain

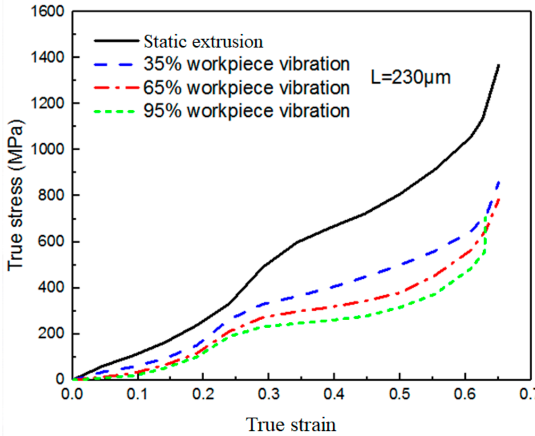

(**f**) Workpiece vibration mode of 230 μm grain

Figure 5. True stress and true strains with different ultrasonic power outputs.

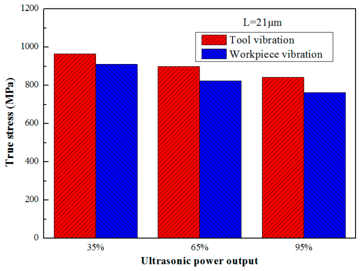

(**a**) 21 μm

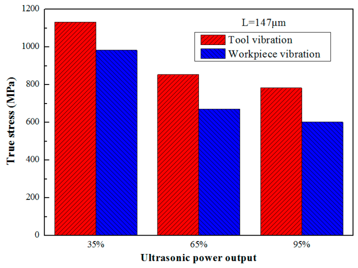

(**b**) 147 μm

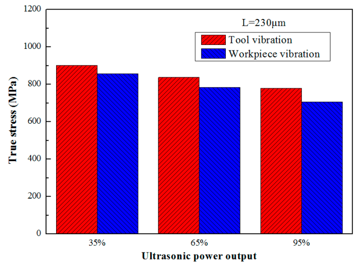

(**c**) 230 μm

Figure 6. Micro-extrusion stress with different power output and different vibration modes for different grain sizes.

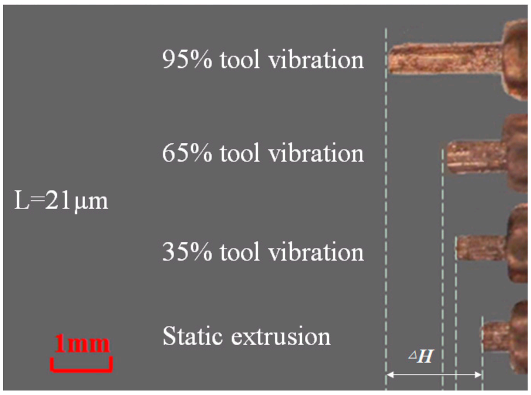

(**a**) Tool vibration mode of 21 μm

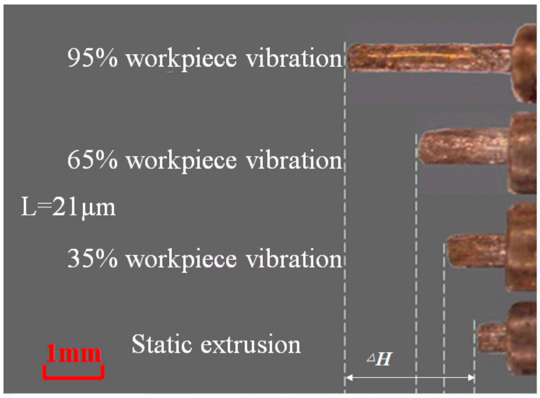

(**b**) Workpiece vibration mode of 21 μm

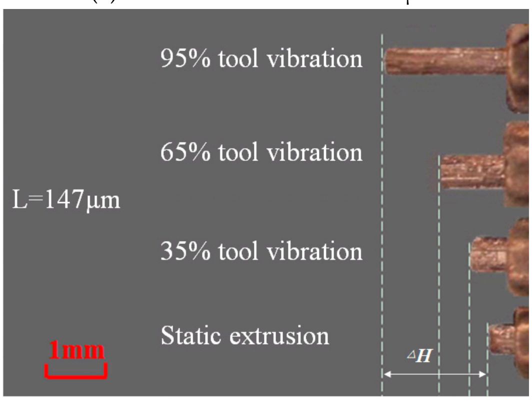

(**c**) Tool vibration mode of 147 μm

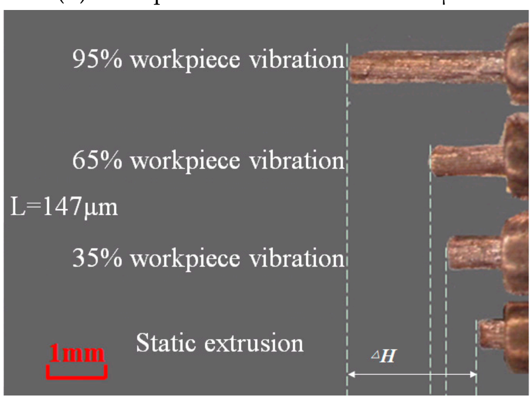

(**d**) Workpiece vibration mode of 147 μm

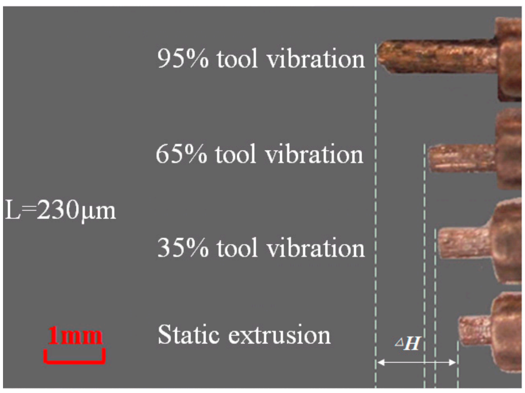

(**e**) Tool vibration mode of 230 μm

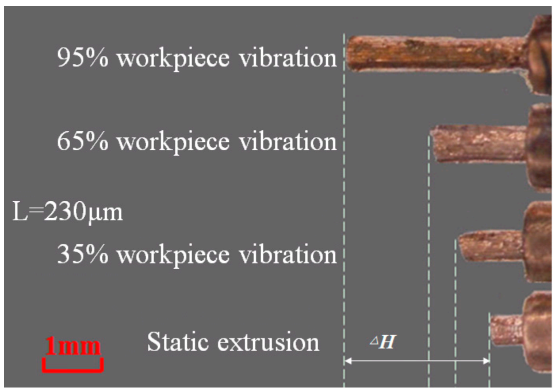

(**f**) Workpiece vibration mode of 230 μm

Figure 7. Micro-extrusion lengths with different ultrasonic power outputs.

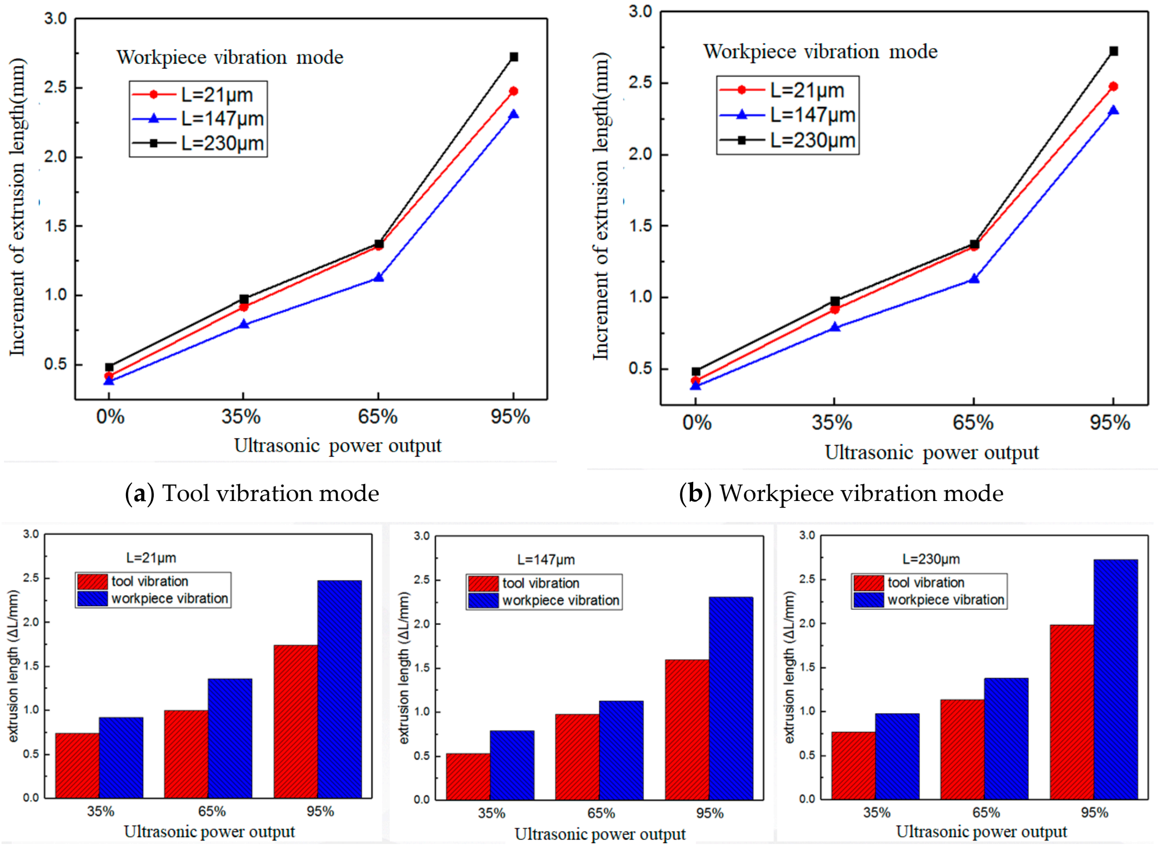

(**a**) Tool vibration mode (**b**) Workpiece vibration mode

(**c**) 21 μm (**d**) 147 μm (**e**) 230 μm

Figure 8. Increment of micro-extrusion length with different ultrasonic power outputs and vibration modes.

3.2. Effect of Copper Grain Size

The results of true stress and true strain and the micro-extrusion lengths of specimen with different grain sizes are shown in Figures 9 and 10. From the figures, we can find that there are marked rise-fall trends both for true stress and micro-extrusion length with grain size increasing under all extrusion conditions including tool vibration, workpiece vibration and static extrusion. For example, the maximum true stress of static extrusion increases from 1367.77 MPa to 1500.71 MPa and then reduced to 1467.98 MPa when the initial copper specimen grain size increases from 21 μm to 147 μm and 230 μm (as shown in Figure 9g). Meanwhile, the micro-extrusion lengths appears with an obvious shape of V in Figure 10d,e, wherein the extrusion length of 95% workpiece vibration reduces from 2.48 mm to 2.31 mm and then increases to 2.73 mm when the initial copper specimen grain size increases from 21 μm to 147 μm and 230 μm. Therefore, the copper specimen with grain size L = 147 μm can take a maximum true stress and take a minimum extrusion length under all extrusion conditions including tool vibration, workpiece vibration and static extrusion. The significant size effect phenomena of different grain sizes are appeared to affect the micro-extrusion ability of copper T2.

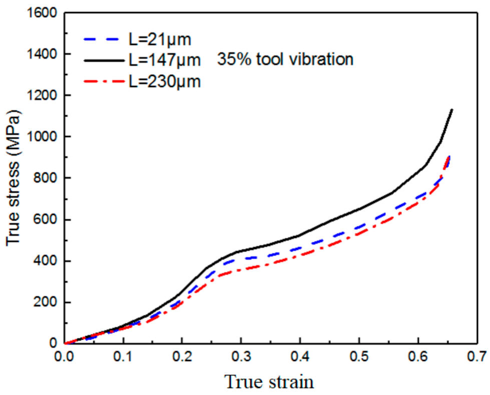

(**a**) 35% tool vibration

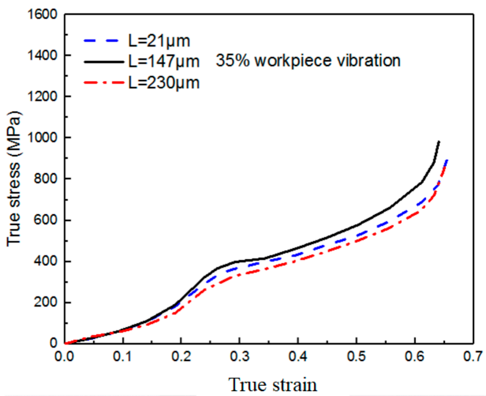

(**b**) 35% workpiece vibration

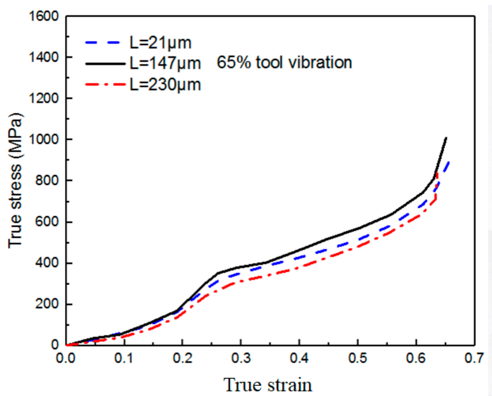

(**c**) 65% tool vibration

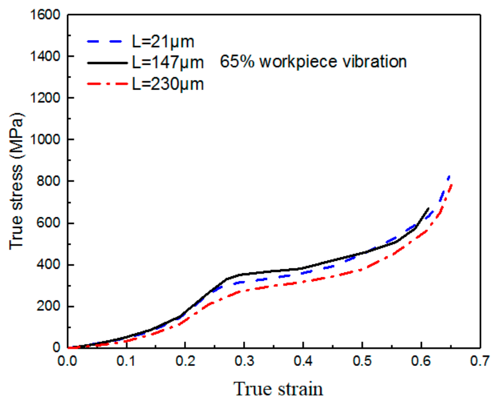

(**d**) 65% workpiece vibration

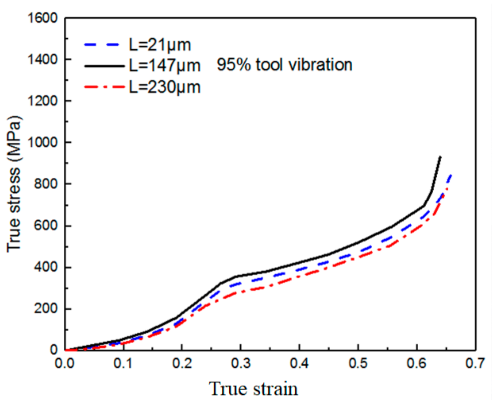

(**e**) 95% tool vibration

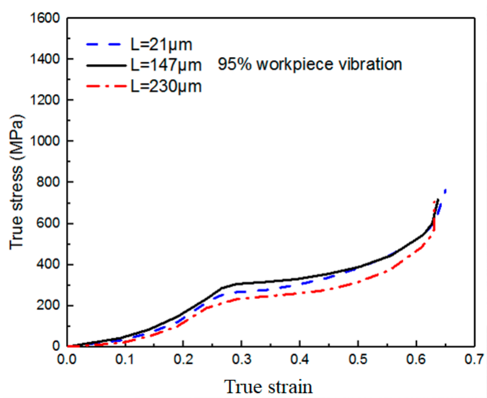

(**f**) 95% workpiece vibration

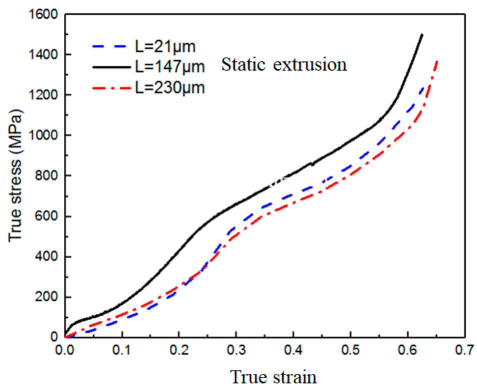

(**g**) static extrusion

Figure 9. True stress and true strains with different initial grain sizes.

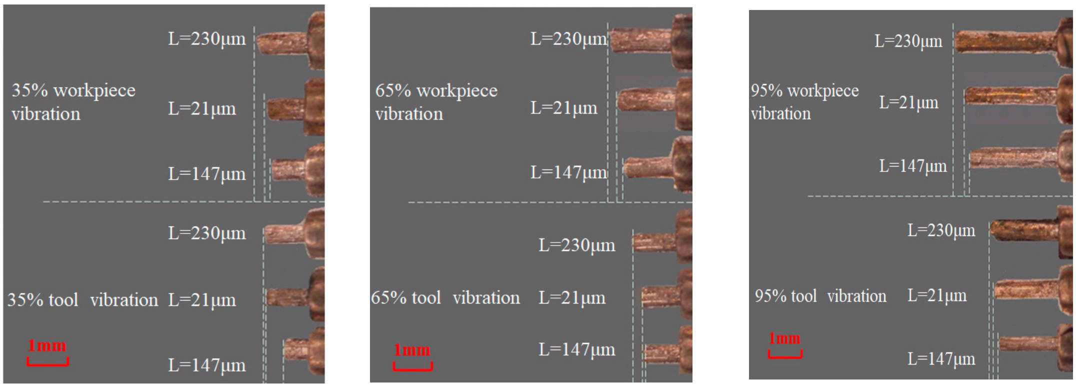

(a) 35% power output (b) 65% power output (c) 95% power output

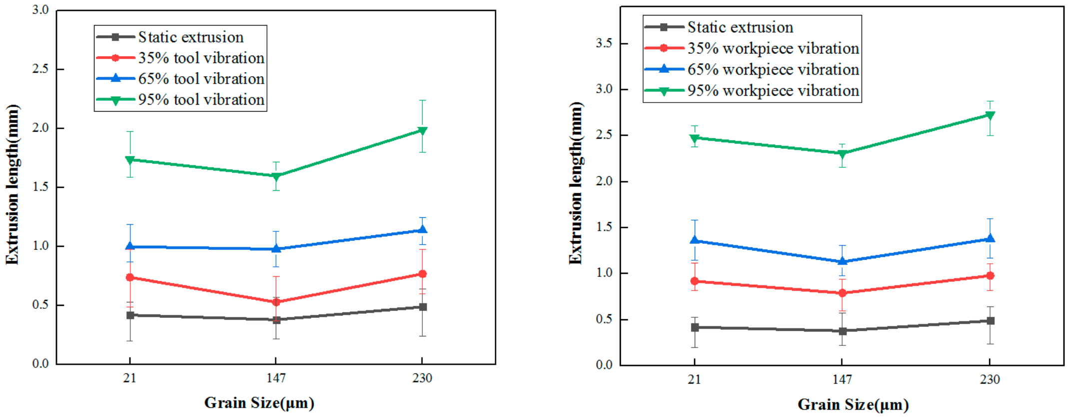

(**d**) tool vibration mode (**e**) workpiece vibration mode

Figure 10. Micro-extrusion lengths with different initial grain size.

3.3. Microstructure Properties of Different Vibration Modes

Microscopic microstructure and micro-hardness on the cross section of extruded copper specimen with different grain sizes are shown in Figures 11 and 12. According to the results, there are many broken fine-grains appeared near grain boundaries with 95% tool vibration and 95% workpiece vibration, where the grain size of broken crystals was smaller than that of static extrusion for all three initial grain sizes. In addition, there are more broken crystals appearing with workpiece vibration mode than that with tool vibration mode (shown in the areas with red circles in Figure 11a–i). On the other hand, the micro-hardness of the copper specimen cross section also increased with the increasing of ultrasonic power output with both tool and workpiece vibration modes, wherein the micro-hardness with workpiece vibration is small lightly higher than that of tool vibration (shown in Figure 12a–c).

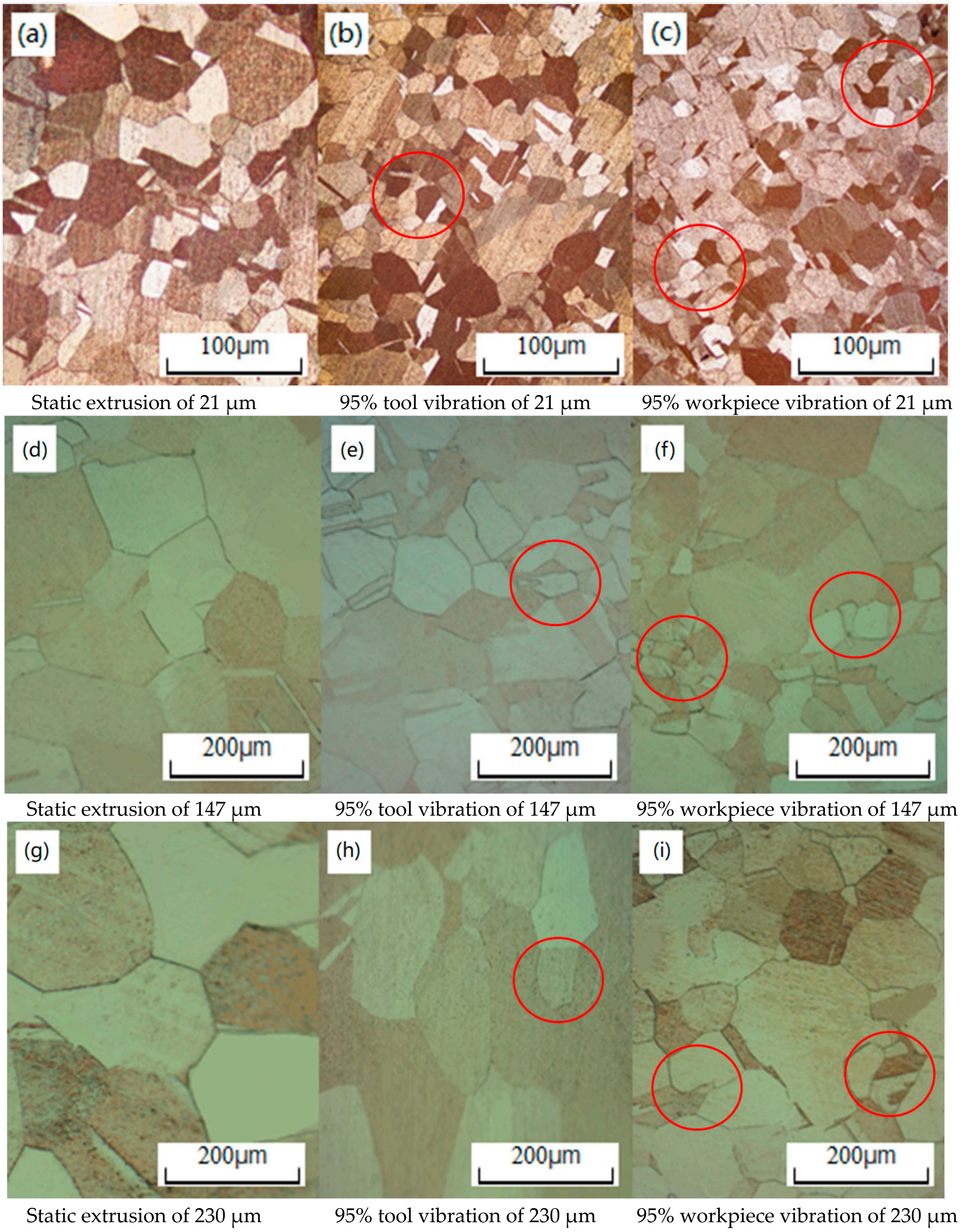

Figure 11. Microscopic microstructure of micro-extruded specimen with different vibration modes.

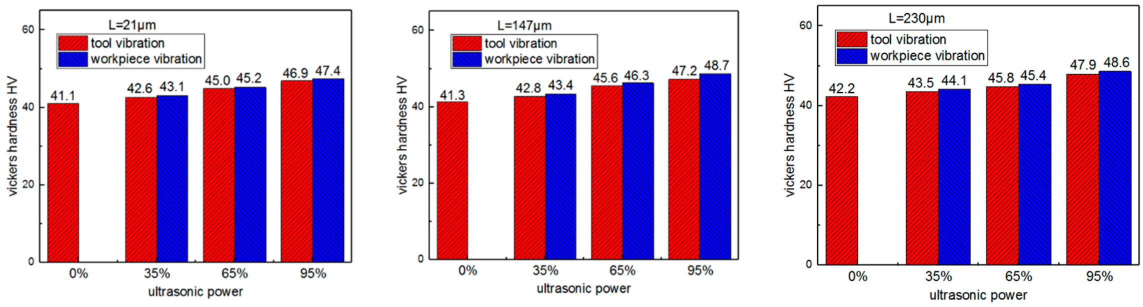

(**a**) 21 μm (**b**) 147 μm (**c**) 230 μm

Figure 12. Cross section micro-hardness of micro-extruded specimen with different vibration modes.

3.4. Discussions

3.4.1. Ultrasonic Softening Effect

It is clear from the above experimental results that the ultrasonic workpiece vibration mode can get more improvement to the micro-extrusion properties of T2 copper specimen than the tool vibration mode with the increasing ultrasonic power output, whether on reducing micro-extrusion stress, extending micro-extrusion length, refining the grain size of crystals and enhancing the micro-hardness. These phenomena could be explained with ultrasonic softening effect and ultrasonic energy transmission capacity.

Referring to the researches on ultrasonic micro plastic forming process with tool vibration mode [17,18], the effect of ultrasonic tool vibration on metal plastic deformation can be explained by stress superposition, acoustic softening and friction decrease. Furthermore, the model for predicting reduction of yield stress under the excitation of ultrasonic tool vibration can be supposed as follows:

$$\Delta\sigma_s = \Delta\sigma_t + \Delta\sigma_p + \Delta\sigma_f \quad (1)$$

where $\Delta\sigma_s$ is the total reduction of yield stress, $\Delta\sigma_t$ is the yield reduction due to acoustic softening, $\Delta\sigma_p$ is the yield reduction due to stress superposition, $\Delta\sigma_f$ is the yield reduction due to friction decrease.

The stress reduction due to acoustic softening $\Delta\sigma_t$ can be expressed as [18]:

$$\Delta\sigma_t = -\beta M\hat{\tau}(E/\hat{\tau})^m \quad (2)$$

where β and m are parameters to be determined in experiments, M is the Taylor factor, $\hat{\tau}$ is the mechanical threshold of material, E is the acoustic energy density, can be expressed as follows [18]:

$$E = \alpha_t {\xi_t}^2 {\omega_t}^2 \rho_t = {\xi_w}^2 {\omega_w}^2 \rho_w \quad (3)$$

$$\alpha_t = 4\rho_t c_t \rho_w c_w / (\rho_t c_t + \rho_w c_w)^2 \quad (4)$$

where ρ_t and ρ_w are the material density of tool and workpiece, c_t and c_w are the wave speed for tool and workpiece, α_t is the energy transmission coefficient between different materials, ξ_t, ξ_w and ω_t, ω_w are vibration amplitude and angular frequency of too and workpiece respectively.

According to the Equations (2)–(4), it is clear that the energy transmission coefficient α_t of ultrasonic tool vibration mode is usually less than one, in which the ultrasonic energy transmitted and absorbed by workpiece should be less than the ultrasonic energy output of tool. Some energy must be lost during the transmission process. In this paper, the copper specimen was excited by different modes (tool vibration mode and workpiece vibration mode). In the tool vibration mode, the end face of extrusion tool touched the upper surface of cylindrical copper specimen by high-frequency tapping, the energy transmission process of which is similar to the condition of Equations (2)–(4). On the other hand, in the workpiece vibration mode, the workpiece vibrates as a whole with the extrusion mold under the pre-pressure action and make active high-frequency impact with the extrusion tool. So it can be concluded that the energy transmission coefficient α_w between extrusion mold and copper specimen should be infinitely close to one and obvious greater than the energy transmission coefficient α_t of ultrasonic tool vibration mode. Therefore, the ultrasonic energy absorbed by specimen in workpiece vibration mode should be higher than that in tool vibration mode, which means the workpiece vibration mode can get stronger ultrasonic softening effect than the tool vibration mode by higher ultrasonic energy transmission capacity. As for the $\Delta\sigma_p$ and $\Delta\sigma_f$, the stress superposition and friction decrease effect in the micro-extrusion process between tool and specimen are at the same condition whether in tool vibration mode or in workpiece vibration mode. Therefore, the different total reduction of yield stress $\Delta\sigma_s$ between tool vibration mode and workpiece vibration mode mainly come from the different yield reduction of acoustic softening.

The stronger ultrasonic softening effect can explain the phenomenon of the lower micro-extrusion stress and larger micro-extrusion length of workpiece vibration mode comparing with tool vibration mode. On the other hand, with the increasing of ultrasonic power output, the tool or workpiece vibration amplitude will be increased at the same time under different ultrasonic vibration modes, which also means higher ultrasonic energy. Therefore, the higher ultrasonic softening effect can be generated with high ultrasonic power output, which can also explain the phenomena of maximum reduction of stress and longest extrusion length with 95% ultrasonic power output in Figures 6–8. As for grain refining and micro-hardness improvement, it can also be explained with the higher percentage absorption of ultrasonic energy in workpiece vibration mode, the higher ultrasonic energy can enhance the grain refining process and get higher micro-hardness.

3.4.2. Grain Size Effect

Experiment results also show that both the micro-extrusion true stress and the micro-extrusion length (EL) tend to increase first and then decrease with the increasing of grain sizes, which can be explained by the V type hole micro extrusion forming model in Figure 13. The diameter of V type hole is varying from 0.5 mm to 0.4 mm. The extrusion forming factor D/L (D is the extrusion diameter and L is the grain size) is designed to represent the number of grains in deformation zone. When L = 21 μm, the value of D/L is 19.0–23.8. When S increases to 147 μm and 230 μm, the value of D/L reduces to 2.72–3.40 and 1.74–2.17.

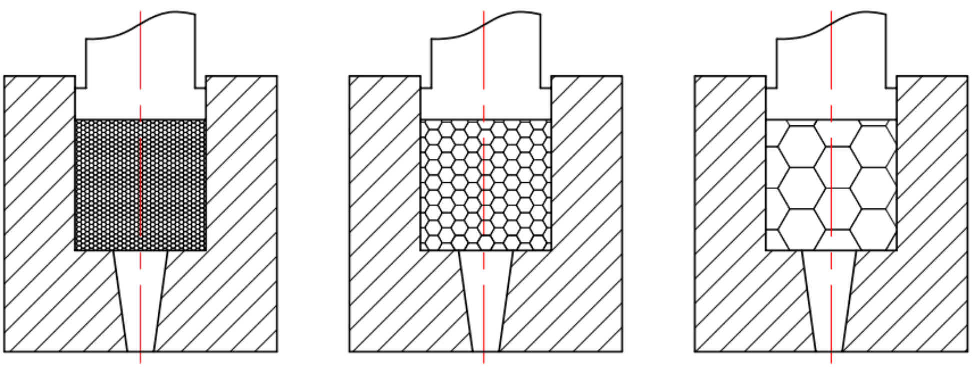

(**a**) Multi-grains extrusion (**b**) 2–3 grains extrusion (**c**) 1–2 grains extrusion

Figure 13. Schematic diagram of V type hole micro extrusion forming models with different extruded grains.

According to the Hall-Petch equation: $\sigma_y = \sigma_0$ + kL − 1/2 (σ_y is yield stress, k is material constant and L is everage grain size), the deformation resistance should be greater with the grain size is smaller. In this paper, when L is 21 μm and D/L is 19.0–23.8, the micro-extrusion process can be regarded as a multi-grain homogeneous deformation process (shown in Figure 13a). When L is increased to 147 μm and D/L is 2.72–3.40, the number of grains in deformation zone is only about 3 (shown in

Figure 13b). The micro-inhomogeneity of copper sample will bring the inhomogeneous deformation increment of grain interior and grain boundary. Therefore, the grains in soft orientation decrease and the deformation coordination among grains becomes much more difficult, the stress concentration and the resistance of micro-extrusion deformation increase greatly. When L is 230 μm and D/L is 1.74–2.17, the micro-extrusion process is close to single crystal deformation (shown in Figure 13c). Very small number of grains will increase the proportion of surface grains and the constraint and grain boundary strengthening effect of which are smaller than that of inner grains. In this case, the blocking effect of grain boundary and dislocation is greatly reduced, while the deformation resistance of grains can also decrease, and the additional ultrasonic energy is enough to make copper material get better micro-extrusion characteristic [19]. In a word, when the number of forming grains in deformation zone reduces to about three, the ultrasonic micro-extrusion process becomes difficult with the grain size effect of micro-forming. When the number of forming grains in deformation zone is about two, the micro-forming size effect of T2 copper material can be improved with assisted ultrasonic vibration, while the higher ultrasonic energy of workpiece vibration mode can get greater micro-forming ability than the tool vibration mode.

4. Conclusions

In this paper, the ultrasonic vibration of tool and workpiece was applied by a self-developed ultrasonic vibration system and press machine and the micro-extrusion characteristic of copper T2 was studied with different ultrasonic vibration modes. The conclusions are as follows:

1. The ultrasonic vibration system and plastic forming press machine with porous sonotrode realized micro-extrusion process with ultrasonic vibration of tool or workpiece, respectively.
2. The ultrasonic micro extrusion process with the workpiece vibration mode had better ultrasonic energy transmission and absorption capacity, which made the micro forming characteristics of copper T2 better than that of tool vibration mode.
3. The ultrasonic vibration assisted energy helped to improve the grain size effect on double crystal scale micro-extrusion process of copper T2, in which the workpiece vibration mode usually obtained better micro-forming ability than that of tool vibration mode.

Author Contributions: Conceptualization, G.H. and L.X.; writing—original draft preparation and methodology, Y.L. and H.Z.; investigation and data curation, Y.L., Z.Z. and Y.S.; writing—review and editing, G.H. and L.X.

Funding: This research was funded by Research Subject of State Key Laboratory of Mechanical System and Vibration, (No. MSV-2019-10), the Open Research Fund Program of Shanxi Key Laboratory of Non-Traditional Machining (No. 2017SXTZKFJG01) and the National Natural Science Foundation of China (No. 21576240).

Conflicts of Interest: The authors declare no conflicts of interest.

References

1. Sedaghat, H.; Xu, W.X.; Zhang, L.C. Ultrasonic vibration-assisted metal forming: Constitutive modelling of acoustoplasticity and applications. *J. Mater. Process. Technol.* **2019**, *265*, 122–129. [CrossRef]
2. Fu, M.W.; Wang, J.L.; Korsunsky, A.M. A review of geometrical and microstructural size effects in micro-scale deformation processing of metallic alloy components. *Int. J. Mach. Tools Manuf.* **2016**, *109*, 94–125. [CrossRef]
3. Jun, H.; Tetsuhide, S.; Tomoaki, Y.; Tomomi, S.; Ming, Y. Ultrasonic dynamic impact effect on deformation of aluminum during micro-compression tests. *J. Mater. Process. Technol.* **2018**, *258*, 144–154.
4. Lou, Y.; Liu, X.; He, J.S.; Long, M. Ultrasonic-assisted extrusion of ZK60Mg alloy micropins at room temperature. *Ultrasonics* **2018**, *83*, 194–202. [CrossRef] [PubMed]
5. Yao, Z.H.; Kim, G.Y.; Faidley, L.A.; Zou, Q.Z.; Mei, D.Q.; Chen, Z.C. Effects of superimposed high-frequency vibration on deformation of aluminum in micro/meso-scale upsetting. *J. Mater. Process. Technol.* **2012**, *212*, 640–646. [CrossRef]
6. Hung, J.C.; Tsai, Y.C. Investigation of the effects of ultrasonic vibration-assisted micro-upsetting on brass. *Mater. Sci. Eng. A* **2013**, *580*, 125–132. [CrossRef]

7. Bai, Y.; Yang, M. Optimization of metal foils surface finishing using vibration-assisted micro-forging. *J. Mater. Process. Technol.* **2014**, *214*, 21–28. [CrossRef]
8. Azarhoushang, B.; Tawakoli, T. Developing a special block sonotrode for ultrasonic-assisted grinding process. *Int. J. Mechatron. Manuf. Syst.* **2012**, *5*, 165–174. [CrossRef]
9. Daud, Y.; Lucas, M.; Huang, Z.H. Superimposed ultrasonic oscillations in compression tests of aluminium. *Ultrasonics* **2006**, *44*, 511–515. [CrossRef] [PubMed]
10. Bunget, C.; Ngaile, G. Influence of ultrasonic vibration on micro-extrusion. *Ultrasonics* **2011**, *51*, 606–616. [CrossRef] [PubMed]
11. Wang, C.J.; Liu, Y.; Shan, D.J.; Guo, B.; Han, H.B. Investigations on mechanical properties of copper foil under ultrasonic vibration considering size effect. *Procedia Eng.* **2017**, *207*, 1057–1062. [CrossRef]
12. Lu, T.T.; Shen, Y.; Yu, H.P.; Dong, X.H.; Hu, J. Influence of ultrasonic vibration on pure titanium TA1 micro cylinder compression. *J. Plast. Eng.* **2016**, *23*, 14–18. (In Chinese)
13. Zhou, H.Y.; Cui, H.Z.; Qin, Q.H. Influence of ultrasonic vibration on the plasticity of metals during compression process. *J. Mater. Process. Technol.* **2018**, *251*, 146–159. [CrossRef]
14. Han, G.C.; Li, K.; Peng, Z.; Jin, J.S.; Sun, M.; Wang, X.Y. A new porous block sonotrode for ultrasonic assisted micro plastic forming. *Int. J. Adv. Manuf. Technol.* **2017**, *89*, 2193–2202. [CrossRef]
15. Han, G.C.; Peng, Z.; Xu, L.H.; Li, N. Ultrasonic Vibration Facilitates the Micro-Formability of a Zr-Based Metallic Glass. *Materials* **2018**, *11*, 2568. [CrossRef] [PubMed]
16. Lei, Y.L.; Han, G.C.; Sheng, C.J.; Zhang, Z.C. Design of 10kN ultrasonic-assisted plastic forming press machine and experimental research. *J. Beijing Univ. Aeronaut. Astronaut.* **2019**, *45*, 1622–1629. (In Chinese)
17. Yao, Z.H.; Kim, G.Y.; Wang, Z.H.; Faidley, L.A.; Zou, Q.Z.; Mei, D.Q.; Chen, Z.C. Acoustic softening and residual hardening in aluminum: Modeling and experiments. *Int. J. Plast.* **2012**, *39*, 75–87. [CrossRef]
18. Wang, C.J.; Liu, Y.; Guo, B.; Shan, D.B.; Zhang, B. Acoustic softening and stress superposition in ultrasonic vibration assisted uniaxial tension of copper foil: Experiments and modeling. *Mater. Des.* **2016**, *112*, 246–253. [CrossRef]
19. Wang, C.J.; Wang, H.Y.; Xue, S.X.; Chen, G.; Wang, Y.B.; Wang, S.T.; Zhang, P. Size effect affected mechanical properties and formability in micro plane strain deformation process of pure nickel. *J. Mater. Process. Technol.* **2018**, *258*, 319–325. [CrossRef]

© 2019 by the authors. Licensee MDPI, Basel, Switzerland. This article is an open access article distributed under the terms and conditions of the Creative Commons Attribution (CC BY) license (http://creativecommons.org/licenses/by/4.0/).